EGTRIB Journal
JOURNAL OF
THE EGYPTIAN SOCIETY OF TRIBOLOGY
VOLUME 18, No. 4, October 2021, pp. 1 - 13 **ISSN 2090 - 5882**
(Received September 11. 2021, Accepted in final form September 25. 2021) **jest.journals.ekb.eg**

LUBRICANT FILM BEHAVIOR IN SPUR GEARS

[1]Mustafa A. G. A. Salam, [2]Mohamed L. Shaltout, [1]Nabil A. Gad-Allah and [2]Mokhtar O. A. Mokhtar

[1] Manufacturing Engineering Department, Modern Academy for Engineering and Technology, Cairo, Egypt,
[2] Mechanical Design and Production Department, Faculty of Engineering, Cairo University, Giza, 12613, Egypt.

ABSTRACT
The study of gears lubrication has received a great deal of attention in research work for many decades. During gears running, meshing gears' teeth represent a non-conformal lubricated contact situation. Under loading conditions, Hertzian high contact pressure within the contact zone between the meshing gears' teeth is evident. It can develop significant surface stresses and affect lubricant viscosity by increasing it. Meanwhile, during teeth mesh the contact and lubrication behavior are basically influenced by gears kinematics, dynamics, materials properties, and lubricant characteristics. However, a comprehensive understanding of the lubrication behavior during gears mesh is still in need for further investigations. The present analytical approach simulated gears mesh by equivalent rigid discs. A close insight into the mechanism of lubricant film formation has shown that both hydrodynamic and squeeze actions contribute to lubricant film formation. The contribution of squeeze action is more pronounced than that due to hydrodynamic action. The complicated dynamic and contact conditions in gears during power transmission dictate the variation of generated film thickness values between meshing gears' teeth.

KEYWORDS
Gears Lubrication, Gears' Teeth mesh, Lubrication, Squeeze Action, Hydrodynamic Action.

INTRODUCTION
During gears running, meshing gears' teeth represent a non-conformal lubricated contact situation. Under loading conditions, Hertzian high contact pressure within the contact zone between the meshing gears' teeth is evident. It can develop significant surface stresses and affect lubricant viscosity by increasing it. Meanwhile, during teeth mesh the contact and lubrication behavior are basically influenced by gears kinematics, dynamics, materials properties, and lubricant characteristics. Extensive investigations and research work on gears lubrication have been published theoretically and experimentally during the past decades. Most of these efforts considered elasto-hydrodynamic regime of

lubrication (EHL). This regime takes into account mating elements elastic distortion, high induced Hertzian stresses, lubricant hydrodynamic behavior, and lubricant viscosity variation with pressure and temperature [1–3].

Lubricant film thickness in gear tooth contacts was first predicted based on the elasto-hydrodynamic lubrication (EHL) theory under smooth surface, steady-state, and isothermal assumptions, [1 - 3]. Further investigations of discs lubrication proposed a criterion that can justify the use of a quasi-steady solution for analyzing gear lubrication, [4 - 8]. Several analytical approaches and experimental measurements have been proposed for the estimation of the lubricant film thickness in gears, [9 - 11]. Later, a numerical solution of EHL film thickness, friction, and surface temperature for an entire meshing cycle in spur gears, considering dynamic and thermal effects has been developed, [12, 13]. Analysis of lubricant film formation in EHL contacts of different oil bases and different additives has been also investigated, [14]. The performance of squeeze film of non-Newtonian fluid with additives between long cylinder on flat surface has been studied, [15].

A close insight into the gear teeth contact conditions during power transmission, reveals that the generation of the lubricant film between contacting teeth is a function of not only gears elastic properties, teeth geometry and accuracy, gears kinematics, mode of dynamic load and lubricant behavior, but also basically on the time during which teeth contact takes place. In this context, it is expected that lubricant squeeze action would play a paramount roll in keeping a lubricant film between teeth. The present work adopts the solution of Reynold's equation for iso-viscous lubricant and rigid cylindrical discs for unidirectional load in an endeavor towards estimating the lubricant film thickness variation during gears teeth mesh.

KINEMATICS OF MESHING GEARS

The present investigation describes the lubrication behavior between two spur gears' teeth during meshing cycle as being simulated by discs as shown in Fig. A1 in the Appendix. At any point on the line of action the respective two radii of curvature of mating involutes will be present as two rotating cylinders (discs) running at pure rolling and combined rolling and sliding velocities with lubricant film separating them. The proposed parameters of the pair of meshed gears upon which the computations in this paper are based are summarized in Table 1.

To study kinematics of each point of the contact during meshing cycle, several points separated with a specified interval (taken in this work as 1 mm) are selected on the line of action between position N_1 (before the pitch point P_p) and position N_2 (after the pitch point P_p), as shown in Fig. A1 in the Appendix. Consequently, the variation of the radii of the simulated cylinders ρ_1 and ρ_2 can be computed. The calculated variation of the radii of curvature along the line of action are shown in Fig. 1.

Table 1. Parameters of the meshed gears

Parameter	Value
Gear Module, m	4.5 mm
Pressure Angle, α	20o
Gear face-width, L	45 mm
Pinion number of teeth	16
Pinion pitch circle radius, R_1	36 mm
Gear number of teeth	24
Gear pitch circle radius, R_2	54 mm
Center distance	90 mm
Gear material Young's modulus, E	210 GPa
Gear material Poisson's ratio, ν	0.3
Lubricant oil viscosity, μ	0.075 Pa.s

It can be noticed that the equivalent curvature radius ρ_{eq} along the line of contact increases first till it reaches a maximum near the pitch point, then it decreases. The variation of the rolling and sliding velocities along the line of action is illustrated in Fig. 2. From Fig. 2(a), the velocity of the point of contact with respect to gear 1 (pinion) V_1 is decreasing along the line of contact, while the velocity of the point of contact with respect to the gear 2 V_2 is increasing. From Fig. 2(b), the tangential velocity of the point of contact with respect to the pinion V_{t1} is decreasing, while the tangential velocity of the point of contact with respect to the gear V_{t2} is increasing along the line of action. The relative tangential velocity V_t is decreasing along the line of contact, and it is equal to zero at the pitch point. It can be noticed that the equivalent curvature radius ρ_{eq} along the line of contact increases first till it reaches a maximum near the pitch point, then it decreases.

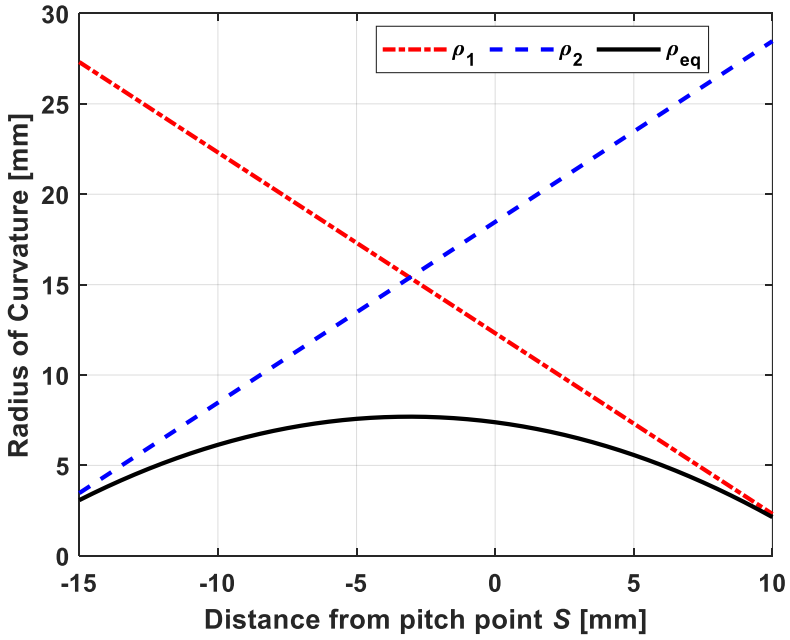

Fig. 1 Variation of the radii of the simulated cylinders along the line of contact.

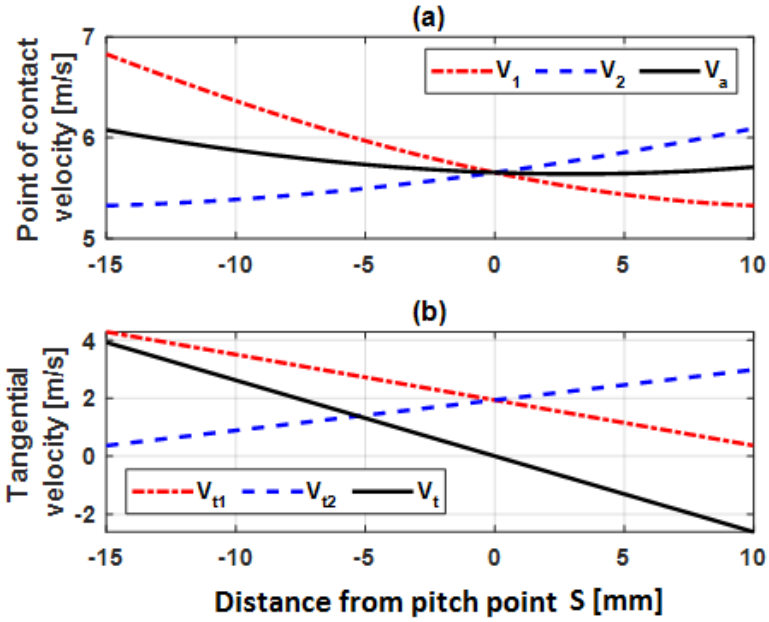

Fig. 2 Variation of the point of contact velocities along the line of contact.

LUBRICANT FILM BEHAVIOR DURING GEAR MESHING

This paper adopts the solution of Reynolds equation for iso-viscous lubricant and rigid bodies under unidirectional variable load. This approach is suitable to describe the lubricant film behavior between gears teeth during meshing cycle. A full description of the geometrical and kinematic features of spur gears are summarized in the Appendix. During gear teeth meshing, a very small elastically deformed contact zone is formed between the gear teeth. Consequently, the lubricant flow (side leakage) parallel to the gear face width (line of contact) is negligibly small and the entire lubricant can be assumed to flow in the direction of teeth motion. Thus, the one-dimensional analysis can be applied to hydrodynamic lubrication of gears. The analysis of gear lubrication is based on the generalized Reynolds equation, where the gear teeth are considered as rigid discs flooded with iso-viscous incompressible lubricant with side leakage effects neglected [16],

$$\frac{d}{dx}\left(\frac{h^3}{\mu}\frac{dp}{dx}\right) = 6(V_1 - V_2)\frac{dh}{dx} + 6h\frac{d}{dx}(V_1 + V_2) + 12\frac{dh}{dt} \qquad (1)$$

where h is the lubricant film thickness and p is the lubricant pressure.

The solution of the above equation gives the pressure distribution in the contact zone which depends on the variation of the lubricant film thickness along the flow direction $\frac{dh}{dx}$ and the variation of the lubricant film thickness with time $\frac{dh}{dt}$. The first and second terms on the right-hand side of Eq. (1) are responsible for the hydrodynamic or wedge action due to the combined effects of rolling and sliding relative motion, while the third term is responsible for the squeeze action along the film thickness direction. By double integration and applying boundary condition, the pressure equation due to hydrodynamic action (wedge action) can be expressed as [17],

$$P_{hyd} = \frac{6\mu V_a}{h_o^2}\sqrt{2\rho_{eq}h_o}\left[\frac{\epsilon}{2} + \frac{\sin 2\epsilon}{4} - \sec^2\epsilon\left(\frac{3}{8}\epsilon + \frac{\sin 2\epsilon}{4} - \frac{\sin 4\epsilon}{32}\right)\right] \quad (2)$$

where h_o is the minimum film thickness and the parameters ϵ and ρ_{eq} are given as,

$$\epsilon = \tan^{-1}\left(\frac{x}{\sqrt{2\rho_{eq}h_o}}\right)$$

$$\rho_{eq} = \frac{\rho_1\rho_2}{\rho_1 + \rho_2}$$

By assuming a film extent of π, the load equation due to wedge action can be represented as [18],

$$W_{hyd} = \frac{2.448\,\mu\,\rho_{eq}\,V_r\,L}{h_o} \quad (3)$$

The pressure equation due to squeeze action due to normal approach of the two meshing teeth can de expressed as [19],

$$P_{sq} = \frac{3\,\mu\,V_n}{h_o+\rho_{eq}}\left(1 - \frac{h_o+\rho_{eq}}{h}\right)^2 \quad (4)$$

By assuming a film extent of π, the load equation due to squeeze action can be represented as [19],

$$W_{sq} = \frac{3\,\pi\,\mu\,\rho_{eq}\,L\,V_n}{h}\sqrt{\frac{\rho_{eq}}{h}} \quad (5)$$

RESULTS AND DISCUSSION

The present investigation was done on a pair of spur gears with the specifications listed in Table 1. In this work, it is intended to study the lubricant film formation between gears teeth meshing along the line of action. To investigate the effect of the position of contact (point M shown in Fig. A1) along the line of action from start to end of meshing, five contact points will be selected for investigation on the line of action. The first point is the pitch point in addition to two points before and two after the pitch point with 3 mm interval. Thus, the distances of the selected points along the line of action with respect to the pitch point will be $\{-6, -3, 0, 3, 6\}$ mm.

The present work considers the important role of normal approach speed compared with peripheral speed. The infinitesimal time of teeth mesh duration available can be sufficient to keep a minimum film thickness under squeeze action, whereas this time may not be sufficient to satisfy time requirement needed for hydrodynamic action to take place. In an endeavor to assess the role that each of the hydrodynamic and/or the squeeze actions may play in dictating the final lubricant behavior, the pressure distribution due to each one has

been developed for an exemplary loaded gear at a load of 0.8 MN and with a film thickness 3 µm, as shown in Fig. 3. The figure shows that the squeeze action renders higher pressure than that due to hydrodynamic action. The pressure generated due to squeeze action (P_{sq}) is more pronounced than that generated from hydrodynamic action (P_{hyd}) as being depicted from pressure distribution shown in Fig. 3. This confirms the postulations that the lubricant film between engaged teeth can be attributed mainly to squeeze action.

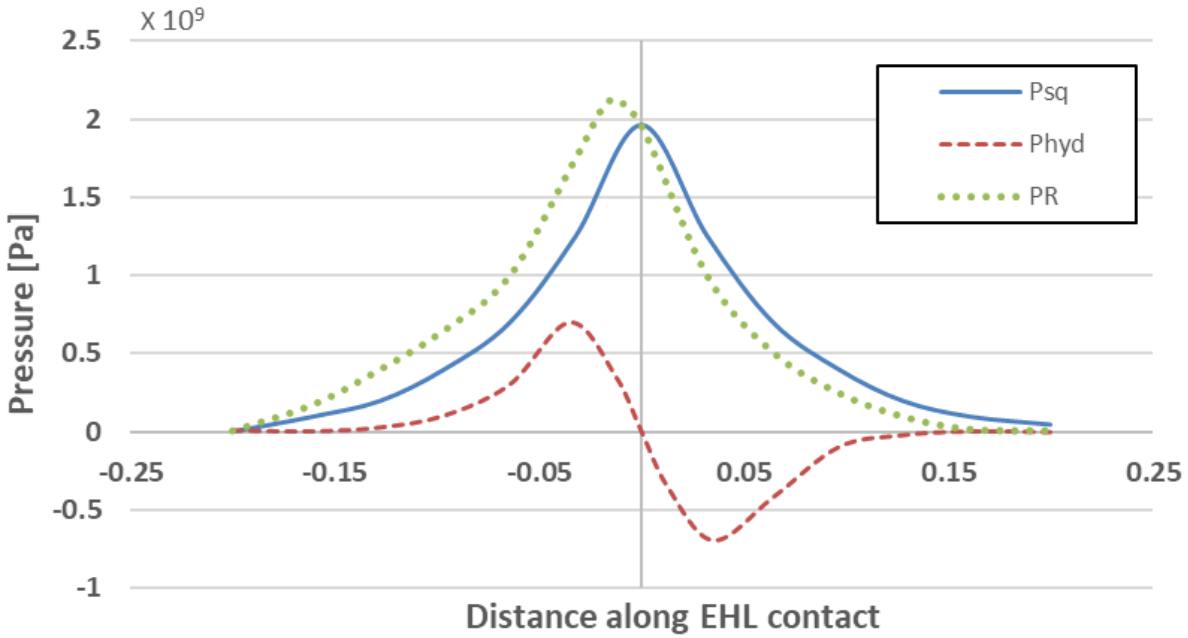

Fig. 3 Pressure distribution due to squeeze and hydrodynamic actions at load 0.8 MN and $h_o = 3\ \mu m$.

The relation between the maximum attained pressure as the sum of both hydrodynamic and squeeze actions and minimum film thickness is presented in Fig. 4. The maximum pressure developed is inversely proportional to values of minimum film thickness at pitch point. This is evident as high pressures due to high applied load would eventually squeeze the entrapped lubricant film between gears teeth leading to a thinner film thickness. The integration of the pressure equation yields the load capacity which is manifested as a relation between applied load and corresponding generated film thickness as shown in Fig. 5. The curves are plotted under conditions related to each point on the path of line of action. The graph indicates an expected inverse proportion between applied load and generated film thickness as depicted in Fig. 4. The trend of behavior shown in the graph comes in line with the previous analytical findings [7, 13].

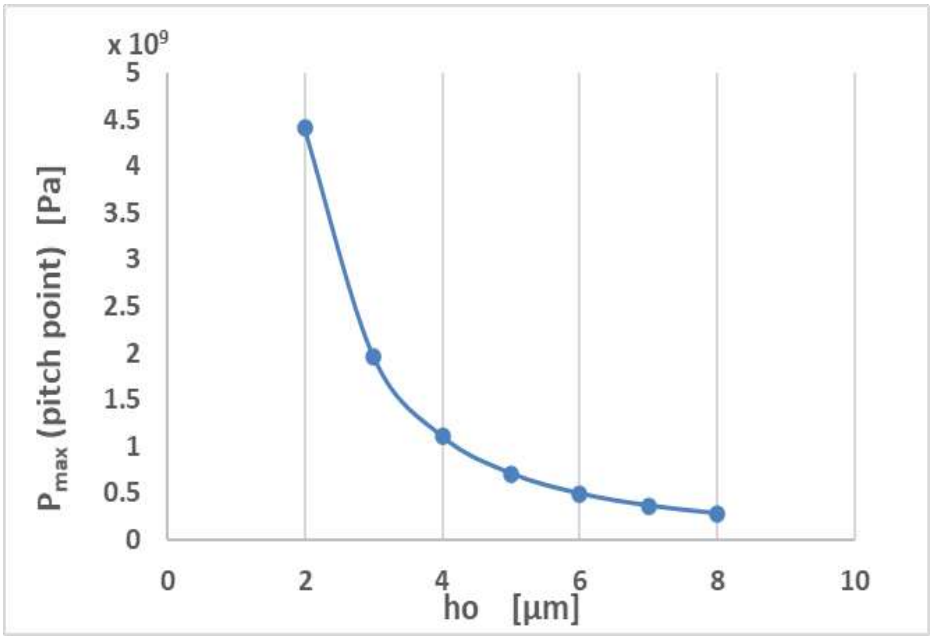

Fig. 4 Maximum overall developed pressure at pitch point against different values of minimum film thickness.

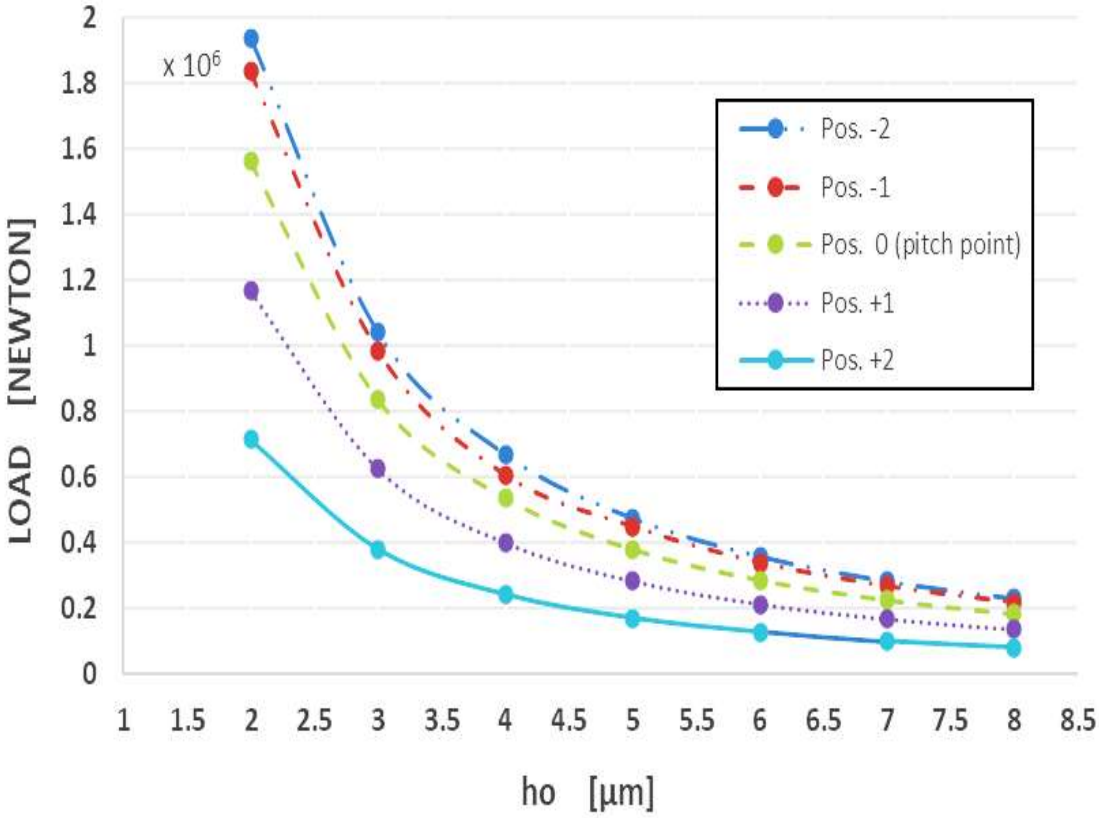

Fig. 5 Values of film thickness at each point on the line of action at different loads.

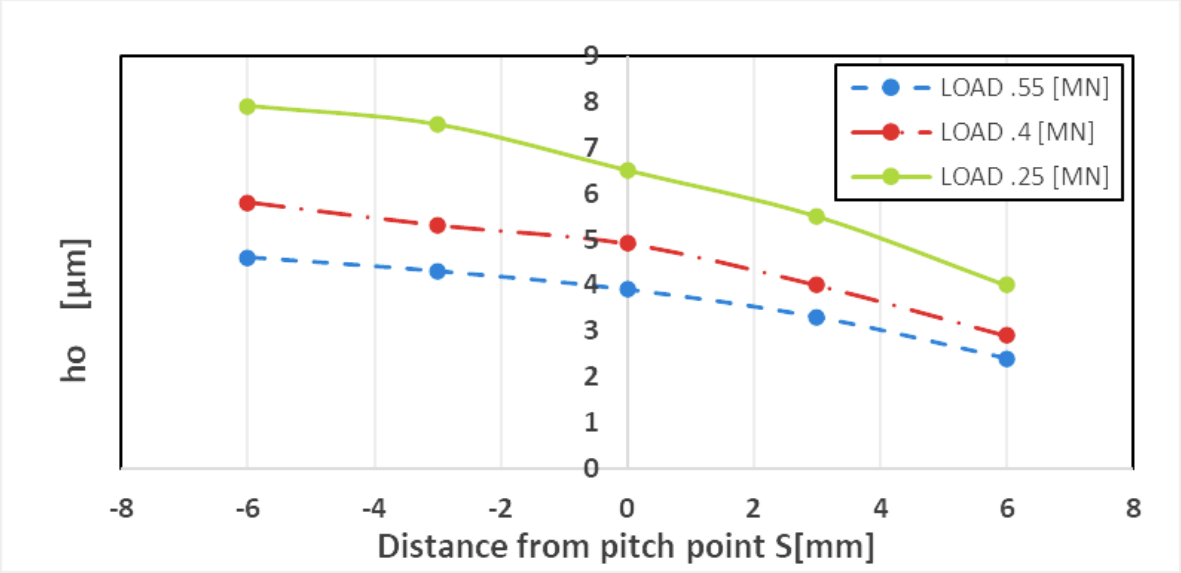

Fig. 6 Film Performance at different loads along action line.

Under the applied load transmitted through gears' teeth, the generated lubricant film thickness varies along the action line from a maximum value at start of teeth contact to a minimum at the end of the contact. Both squeeze action and hydrodynamic effects contribute to film shape formation. The analysis revealed that the contribution of squeeze action due to teeth approach during meshing is more appreciated than the hydrodynamic action. In all previous studies, the gears lubrication has been treated assuming discs with radii analogous to the gears' involutes radii of curvature. The discs are then treated as being rotating under continuously steady state [1-3]. In this case, the normal approach velocity between meshing teeth during an infinitesimal small time has been ignored; for example, a pinion with 20 teeth running at 1500rpm, the time of mesh with mating gear teeth is about 1/500 of a second. This emphasizes that the contribution of squeeze action would be predominant in maintaining a lubricant film between teeth. The geometrical and kinematic characteristics of meshing gears at different points along line of action control the lubrication behavior and hence, dictate the minimum lubricant film thickness. The investigation reveals that largest percent of applied load is carried by squeeze film [9, 10].

In general, applied loads in the range from 0 to 2 MN in the present example, are associated with a change of film thickness throughout the path of line of action up to about 8 µm. This confirms the results came from previous findings [13,16] for iso-viscous lubricant and rigid solids. The performance of film thickness along line of action at any specified load is presented in Fig. 6 which represents the variation of the lubricant film thickness along line of action with the load. These results are in some agreement with the previous finding [13]. The present analysis confirms that squeeze action plays the main roll in describing a film thick decreasing with time through moving along the line of action as shown in Fig. 6. The time taken for the film to drop from a maximum at starting to a minimum at end of line of action is expected to be analogous to that required to squeeze the lubricant film under load. It is worth mentioning that the calculation of gears lubrication behavior based on simulated disc at pitch point may lead to inaccurate

assumptions and results. It is clear the lubricant film my drop by about 50% from start to end of mesh cycle with an average value at pitch point.

CONCLUSIONS

The lubricant film thickness between engaged gear teeth under load has shown to vary during gears mesh along the line of contact. Under loading conditions, the squeeze action may be more pronounced than the hydrodynamic one in generating and maintaining a lubricant film between meshing gears teeth. Results displayed a maximum value of film thickness at the beginning of the gears teeth mesh which declines to lower value at the end of mesh.

REFERENCES

1. Dowson D. and Higginson G. R., "A Numerical Solution to the Elasto-Hydrodynamic Problem", Journal of Mechanical Engineering Science, Vol. 1, No. 1, pp. 6 - 15, (1959).

2. Dowson D., Higginson G. R., and Whitaker A. V., "Elasto-Hydrodynamic Lubrication: A Survey of Isothermal Solutions", Journal of Mechanical Engineering Science, Vol. 4, No. 2, pp. 121 - 126, (1962).

3. Dowson D. and Higginson G. R., "Elasto-hydrodynamic Lubrication: The Fundamentals of Roller and Gear Lubrication", London: Oxford: Pergamon Press; (1966).

4. Herrebrugh K., "Elastohydrodynamic Squeeze Films between Two Cylinders in Normal Approach", Journal of Lubrication Technology, Vol. 92, No. 2, pp. 292 - 301, (1970).

5. Lee K. M. and Cheng H. S., "The Pressure and Deformation Profiles Between Two Normally Approaching Lubricated Cylinders". Journal of Lubrication Technology, Vol. 95, No. 3, pp. 308 - 317, (1973).

6. Dowson D., Markho P. H., and Jones D. A., "The Lubrication of Lightly Loaded Cylinders in Combined Rolling, Sliding, and Normal Motion. Part I: Theory", Journal of Lubrication Technology, Vol. 98, No. 4, pp. 509 - 516, (1976).

7. Markho P. H. and Dowson D., "The Lubrication of Lightly Loaded Cylinders in Combined Rolling, Sliding, and Normal Motion. Part II: Experimental", Journal of Lubrication Technology, Vol. 98, No. 4, pp. 517 - 522, (1976).

8. Gu A., "Elastohydrodynamic Lubrication of Involute Gears", Journal of Engineering for Industry, Vol. 95, No. 4, pp. 1164 - 1170, (1973).

9. Mokhtar M. O. A., "A New Approach to Gears and Cams Lubrication, Part I: Theory; The Performance of Dynamically Loaded Disks", World Symposium on Gears and Gear Transmissions, IFToMM-JuDEKO, Dubrovnik, Yugoslavia, Sept. 13 - 16: 1978, p. Paper No. B - 19/I, (1978).

10. Mokhtar M. O. A., "A New Approach to Gears and Cams Lubrication, Part II: Application; Gears Lubrication", World Symposium on Gears and Gear Transmissions, IFToMM-JuDEKO, Dubrovnik, Yugoslavia, Sept. 13 - 16: 1978, p. Paper No. B - 19/II, (1978).

11. Shawki G. S. A., Mokhtar M. O. A., and Abdel-Ghany A. A., "Experimental investigations into the behavior of elastohydrodynamic lubricating films", Journal of Tribology, Vol. 104, No. 1, pp. 91 - 98, (1982).

12. Wang K. L. and Cheng H. S., "A numerical solution to the dynamic load, film thickness, and surface temperatures in spur gears, Part I Analysis", Journal of Mechanical Design, Transactions of the ASME, Vol. 103, No. 1, pp. 177 - 187, (1981).
13. Wang K. L. and Cheng H. S., "A numerical solution to the dynamic load, film thickness, and surface temperatures in spur gears, Part II results", Journal of Mechanical Design, Transactions of the ASME, Vol. 103, No. 1, pp. 188 - 194, (1981).
14. Hohn B., Michaelis K., and Mann U., "Measurement of Oil Film Thickness in Elastohydrodynamic Contacts Influence of Various Base Oils and Vl-Improvers", Tribology Series, Vol. 31, pp. 225 - 234, (1996).
15. Lin J. R., Liao W. H., and Hung C. R., "The effects of couple stresses in the squeeze film characteristics between A cylinder and a plane surface", Journal of Marine Science and Technology, Vol. 12, No. 2, pp. 119 - 123, (2004).
16. Pinkus O. and Sternlicht B., "Theory of Hydrodynamic Lubrication", McGraw-Hill, New York, (1961).
17. Stolarski T. A., "Tribology in mechanical design", Great Britain: Butterworth-Heinemann, (1990).
18. Khonsari M. M. and Booser E.R., "Applied Tribology: Bearing Design and Lubrication", John Wiley and Sons Ltd, (2008).
19. Popov V. L., "Contact Mechanics and Friction: Physical Principles and Applications", Springer, (2010).

NOMENCLURES

C	**Center distance between pinion and gear [m]**
h_c	**Central oil film thickness [μm]**
h_o	**Minimum oil film thickness [μm]**
L	**Gear face width [m]**
m	**Module of gears**
R_p	**Base circle radius of pinion [m]**
R_g	**Base circle radius of gear [m]**
R_1	**Pitch circle radius of pinion [m]**
R_2	**Pitch circle radius of gear [m]**
R_{L1}	**Radius from center of pinion to any point on the line of action [m]**
R_{L2}	**Radius from center of gear to any point on the line of action [m]**
S	**Distance from any point on the line of action to pitch point**
V_1	**Rolling velocity at any point on the line of action for pinion [m/s]**
V_2	**Rolling velocity at any point on the line of action for gear [m/s]**
V_{Ro}	**Resultant rolling velocity for pinion and gear [m/s]**
V_{n1}	**Normal velocity component at any point on the line of action for pinion [m/s]**
V_{n2}	**Normal velocity component at any point on the line of action for gear [m/s]**
V_{nT}	**Resultant normal velocity for pinion and gear [m/s]**
V_t	**Resultant sliding velocity for pinion and gear [m/s]**
V_{t1}	**Sliding velocity component at any point on the line of action for pinion [m/s]**
V_{t2}	**Sliding velocity component at any point on the line of action for gear [m/s]**
W	**Load carrying capacity carried by squeeze and wedge action [N]**
W_G	**Load carrying capacity carried by wedge action [N]**

W_{sq}	**Load carrying capacity carried by squeeze action [N]**
Z	**Number of teeth**
α	**Pressure angle in degree**
θ_1	**Rolling angle at any point on the line of action for pinion in degree**
θ_2	**Rolling angle at any point on the line of action for gear in degree**
μ	**Lubricant Viscosity [Pa.s]**
ρ_1	**Radius of curvature at any point on the line of action for pinion [m]**
ρ_2	**Radius of curvature at any point on the line of action for gear [m]**
ρ_{eq}	**Equivalent Radius of curvature at any point on the line of action for gears [m]**
ω_1	**Angular velocity of pinion [rad/s]**
ω_2	**Angular velocity of gear [rad/s]**

APPENDIX

GEOMETRY AND KINEMATICS OF INVOLUTE SPUR GEARS

The contact between a pair of involute spur gears can be simulated by the contact between two rigid cylinders of different radii. Along the line of action represented by line $\overline{AE}$ in Fig. A1, the radii of curvature (the equivalent rigid cylinders' radii) ρ_1 and $\rho_2$will vary. The smaller pinion is denoted as gear 1, while the larger gear is denoted as gear 2.

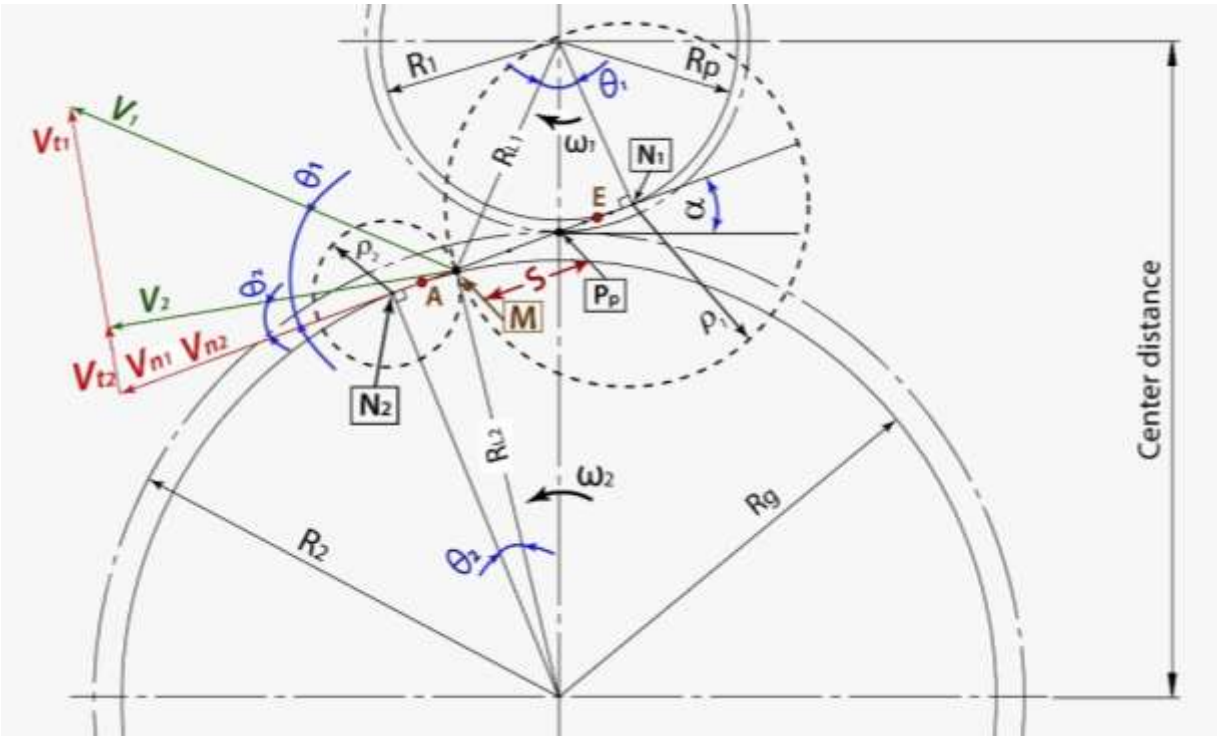

Figure A1 Simulated contact process between two meshed gears.

For any contact point on the line of action (e.g., contact point *M* in Fig. A1), the radii of the approximate rigid cylinders ρ_1 and $\rho_2$can be defined as,

$$\boldsymbol{\rho_1 = \sqrt{R_{L1}^2 - R_p^2}} \quad \textbf{(A-1a)}$$

$$\boldsymbol{\rho_2 = \sqrt{R_{L2}^2 - R_g^2}} \quad \textbf{(A-1b)}$$

where R_{L1} and R_{L2} are the radii of rotation of the contact point with respect to the pinion and gear centers, can be represented respectively as,

$$\boldsymbol{R_{L1} = \sqrt{R_1^2 \pm 2R_1 S \sin\alpha + S^2}} \quad \textbf{(A-2a)}$$

$$\boldsymbol{R_{L2} = \sqrt{R_2^2 \mp 2R_2 S \sin\alpha + S^2}} \quad \textbf{(A-2b)}$$

where $R_1$and $R_2$are the pitch circle radii of the pinion and the gear, respectively. The distance between any contact point on the line of action and the pitch point is denoted as S and the pressure angle is denoted as α. The equivalent curvature radius ρ_{eq} through the line of contact can be represented as,

$$\boldsymbol{\rho_{eq} = \frac{\rho_1 \rho_2}{\rho_1 + \rho_2}} \quad \textbf{(A-3)}$$

From Fig. A1, the rolling angles of the pinion and the gear can be defined as follows,

$$\boldsymbol{\cos\theta_1 = \frac{R_p}{RL_1}} \quad \textbf{(A-4a)}$$

$$\boldsymbol{\cos\theta_2 = \frac{R_g}{RL_2}} \quad \textbf{(A-4b)}$$

Consequently, the respective instantaneous velocities of the point of contact with respect to the pinion and the gear can be represented as,

$$\boldsymbol{V_1 = R_{L1}\omega_1} \quad \textbf{(A-5a)}$$

$$\boldsymbol{V_2 = R_{L2}\omega_2} \quad \textbf{(A-5b)}$$

where ω_1 and ω_2 are angular velocities of pinion and gear, respectively. The point of contact velocity can then be resolved in normal and tangential directions,

$$\boldsymbol{V_{n1} = V_1 \cos\theta_1} \quad \textbf{(A-6a)}$$

$$\boldsymbol{V_{n2} = V_2 \cos\theta_2} \quad \textbf{(A-6b)}$$

The tangential components of velocities are responsible for the sliding action between the teeth of the pinion and the gear,

$$\boldsymbol{V_{t1} = V_1 \sin\theta_1} \quad \textbf{(A-7a)}$$

$$V_{t2} = V_2 \sin \theta_2 \quad \textbf{(A-7b)}$$

The relative sliding velocity at the point of contact can then be determined as follows,

$$V_t = V_{t1} - V_{t2} \quad \textbf{(A-8)}$$

The resultant normal velocity at the point of contact can be defined as,

$$V_n = V_{n1} + V_{n2} \quad \textbf{(A-9)}$$

The mean velocity of the point of contact can be determined as follows,

$$V_a = \frac{V_1 + V_2}{2} \quad \textbf{(A-10)}$$